

Synoptic and Dynamical Characteristics of Severe Cyclonic Storm ASANI May 2022

ABSTRACT:

The synoptic and dynamical conditions for the genesis and intensification of tropical cyclone Asani are clearly highlighted in the present paper. The observationally favourable conditions for the genesis of Asani are high SST, 200 hpa STWJ, and weak vertical shear of horizontal wind, which enhanced the convection and intensified the system. The SCS Asani entered a region with lower SST and lower ocean heat content, causing it to weaken into a deep depression in the Bay of Bengal before making landfall. Because of the anticyclone over Indian landmass, Asani remained within 50 km of the coastline for the entire day; as a result, the system moved slowly and remained nearly stationary. The slow movement led to upwelling of sea water and rainfall over the sea, leading to further cooling of the sea surface. There was also land interaction, thereby increasing friction for a longer period. There was a cold and dry air incursion from the Indian Land region in the middle and upper troposphere, leading to weakening.

Keywords: SST, warm dry winds, ridge, ocean heat content, surface latent heat flux.

1. INTRODUCTION

Tropical cyclones are the most infamous weather events in the world, and they fall into the category of extremely dangerous weather events. Their landfalls can result in human casualties, building damage, and economic losses across the world (Simpson et al., 2002; Pielke and Pielke, 1997). They are large-scale rotating storms that arise over warm tropical ocean waters (Montgomery and Ferrel, 1993). Cyclones that appear in the Bay of Bengal (BoB) and the Arabian Sea and recur in the premonsoon and postmonsoon seasons mostly impact India. These cyclones essentially migrate from the west to the northwest (Chinchole and Mohapatra, 2017). These cyclones have a typical life cycle of 4-6 days. The average frequencies of these cyclones over the BoB and the Arabian Sea are 4 and 1, respectively (Mohapatra et al., 2014b). An early prediction regarding the genesis, development, and tracking of these systems can save many lives.

According to the earlier studies, tropical cyclones mainly develop over the warm ocean with Sea Surface Temperatures (SST) above 26 °C (Palmen, 1948), decreased vertical shear of horizontal wind (Gray, 1968), increased low-level moisture content, and enhanced latent and sensible heat fluxes from the sea surface to the marine boundary layer. Many scientists have also argued that the genesis and development of tropical cyclones are dependent on nearly classic baroclinicity (Bosart and Bartlo, 1991), the interaction of easterly waves or other low-level disturbances with tropical upper tropospheric disturbances (Ramage, 1959; Sadler, 1976; Montgomery and Ferrel, 1993), the Rossby wave energy dispersion of a preexisting typhoon (Li and Fu, 2006). This shows that the genesis and development process of a tropical cyclone is very complex and depends on many factors.

Recently, severe cyclonic storm Asani, which originated in the BoB, caused serious destruction in the coastal districts of Andhra Pradesh state and Tamil Nadu state. According to the India Meteorological Department (IMD), it was a marginal cyclone that occurred in the BoB. The landfall of this cyclone occurred over Andhra Pradesh as a deep depression, causing major damage to agriculture. This is the rarest cyclone to form in the month of May; its track and movement change from time to time and weaken within one day. In this study, the synoptic and dynamical characteristics that contributed to the formation, intensification, and weakening of SCS Asani are investigated. In particular, the impact of synoptic-scale factors such as upper-level dynamic factors like 850, 700, 500, and 200 hpa wind analysis, the sub-tropical Westerly Jet (STWJ), and thermodynamic factors such as the K index, precipitable water, surface energy fluxes, CAPE, total column liquid water content, SST, wind shear, and divergence are analysed.

Objectives

1. To study the factors that enhanced the intensification of SCS Asani.
2. To study the factors that are leading to the weakening of SCS Asani in the Bay of Bengal.
3. To study the factors that influence the change of track from the normal direction.

2. STUDY AREA AND DATA

The study area is primarily India and the North Indian Ocean (NIO) region, spanning between (00 N and 30 N and 50 E and 110 E, respectively, with a particular emphasis on the BoB region (0 O and 30 O and 80 O and 110 O, respectively). IITM, GFS, Wyoming University data, hourly 0.250X 0.250 resolution European Center for Medium Range Forecasts (ECMWF) ERA5 reanalysis data

(Hersbach and Dee, 2016), for various parameters including wind speed direction, temperature, vertical velocity, divergence, specific humidity, and geopotential at different pressure levels, MSLP, SST, surface latent heat flux, surface sensible heat flux, CAPE, column liquid water. Observed track data for SCS Asani has been collected from RSMC New Delhi.

3. DESCRIPTION OF LIFE PERIOD

At 0830 hrs IST on May 6, 2022, a low-pressure area formed over the South Andaman Sea and the adjoining Southeast Bay of Bengal. It was a well-defined low-pressure area over the Southeast Bay of Bengal and the adjoining south Andaman Sea at 0530 IST on May 7. Under favourable environmental conditions, it intensified into a depression over the same region around noon (1130 hrs IST) on the same day. It moved north-westward and intensified into a deep depression over the same area in the evening (1730 hrs IST) on the 7th of May. Continuing to move north-westwards, it intensified into the cyclonic storm "ASANI" in the early morning hours of May 8 (0530 hrs IST) and into a severe cyclonic storm in the same evening (1730 hrs IST) over the southeast Bay of Bengal. It continued to move north-westwards, reaching a peak intensity of 55 knots (100-110 kmph with gusts to 120 kmph) early on the 9th at 0530 IST. It remained at its peak intensity until 10 a.m., or around 1130 hrs. IST, for 30 hours. It began gradually moving north-northwestward on the 10th evening and weakened into a cyclonic storm over the west-central Bay of Bengal about 60 km south-southeast of Machilipatnam in the early hours (0230 hrs IST) of May 11. After that, it moved slowly northward before collapsing into a deep depression over the west central Bay of Bengal near the Andhra Pradesh coast in the evening of May 11 (1730 h IST). It crossed the Andhra Pradesh coast near Machilipatnam during 1730–1930 hours IST on May 11, 2022, as a deep depression with a maximum sustained wind speed of 55–65 kmph, gusting to 75 kmph (IMD bulletins). It then moved slowly west-southwestward and weakened into a depression in the early morning 0530 hrs IST and further into a well-marked low-pressure area in the morning 0830 hrs IST of May 12th over coastal Andhra Pradesh.

4. BRIEF DESCRIPTION OF IMPORTANT PARAMETERS

4.1 Sub-Tropical Westerly Jet (STWJ)

According to the WMO, a "jet stream" is a strong, narrow current concentrated along a quasi-horizontal axis in the upper level troposphere or in the stratosphere characterised by strong vertical and lateral wind shears featuring one or more velocity maxima. STWJ is one of the most important jet streams, and the mean position of this jet stream over the Indian subcontinent is at 27°N at a height of about 12 km (200 hpa). This jet is caused by the concentration of the horizontal temperature gradient below the jet level and the reversal of the gradient above the jet level. This is a large scale feature of the upper air circulation with a high-speed core that can be distinguished from the general wind current. This jet is located near the poleward boundary of the Hadley cell. There is a downstream strengthening of the wind speed in this jet stream. It is seen that, in association with the high-speed centres along the jet axis, there is upper air divergence in the left entrance and right exit sectors. The wind speed of Jet 200 hpa has been calculated.

4.2 Wind Shear

The speed and direction of the wind are different at different heights (pressure levels). Generally, wind speed increases with height. Shear = velocity of wind at upper level minus velocity of wind at lower level is used to calculate vertical shear of horizontal wind. Here, wind shear between 200 and 1000 hpa has been taken into consideration.

4.3. Divergence

This parameter is the horizontal divergence of velocity. It is the rate at which air is spreading out horizontally from a point, per square meter. This parameter is positive for air that is spreading out, or diverging, and negative for the opposite, for air that is concentrating, or converging (convergence). The 200 hpa mean divergence of all synoptic hours for each day has been shown here.

4.4 Vertical velocity (ω)

This parameter is the speed of air motion in the upward or downward direction. Negative values of vertical velocity indicate upward motion. It can be expressed as follows:

$$\omega = - dp/dt$$

where dp/dt is the rate of change of pressure.

4.5 CAPE

This is an indication of the instability of the atmosphere and can be used to assess the potential for the development of convection, which can lead to heavy rainfall, thunderstorms, and other severe weather. This is the potential energy represented by the total excess buoyancy. The larger positive CAPE value indicates greater instability.

4.6. Surface heat fluxes

Surface latent heat flux is the transfer of latent heat (resulting from water phase changes such as evaporation and condensation) between the Earth's surface and the atmosphere through the effects of turbulent air motion. The magnitude of sensible heat flux is governed by the difference in temperature between the surface and the overlying atmosphere, wind speed, and surface roughness. Surface heat fluxes are positive downwards and negative upwards.

4.7. Column rainwater and liquid water content

Total column rainwater is the total amount of water in droplets of various sizes (which can fall to the surface as precipitation) in a column extending from the surface of the earth to the top of the atmosphere. Total column liquid water content is the amount of liquid water contained within cloud droplets in a column extending from the surface of the Earth to the top of the atmosphere. Raindrops, which are much larger in size and mass, are not included in this parameter.

4.8. Total energy vertical integral

This is the vertical integral of total energy for a column of air extending from the surface of the Earth to the atmosphere. Total atmospheric energy is made up of internal, potential, kinetic, and latent energy. This is expressed in joule/m².

4.9. Upper-level trough

The trough is an elongated region of relatively low atmospheric pressure without a closed isobaric contour that would define it as a low-pressure area. The trough may be near the surface or above it. Upper-level troughs reflect cyclonic filaments of vorticity. Their motion induces upper-level wind divergence. The interaction with a cyclonic system can influence and guide the system. The trough at a particular level can be found by plotting the geopotential at that particular level.

4.10 index elevation

It is a measure of the thermal stability of the atmosphere at 500 hPa and is expressed in terms of parcel temperature and environmental temperature (Means 1952).

$T_{500} - T_{\text{parcel}}$ equals LI(K).

Where T_{500} is the environmental temperature at 500 hPa and T_{parcel} is the temperature, it is lifted from 500 m above the surface with the average temperature, pressure, and dew point temperature.

4.11 TTI

This index is useful for estimating storm strength, but it ignores latent instability below 850 hPa (Miller 1972).

$$\text{TTI(K)} = T_{850} - T_{500} + T_{d850} - T_{500}$$

4.12 SWEAT

This index was proposed by Miller in 1972 for determining severe weather.

$$\text{SWEAT} = 12 T_{d850} + 20 (\text{TTI} - 49) + 2 F_{850} + 125 [\sin(d_{500} - d_{850})] + 0.2$$

Where f_{850} , f_{500} are the wind speeds in knots at 850 and 500 hpa, respectively, and d_{500} , d_{850} are the wind direction in 0-360° at 500 and 850 hpa, respectively.

4.13 KI

This index is used for determining the air mass of thunderstorms. It consists of moisture at 850 and 700 hPa and a temperature difference of 850 and 500 hPa. (George 1960)

$$T_{850} - T_{500} + T_{d850} - T_{700} - T_{d700} = \text{KI(K)}$$

4.14 CAPE

It represents the vertically integrated positive buoyancy of an adiabatically rising parcel (Moncrieff and Miller, 1976). Williams and Renno (1993) employed CAPE to study the conditional instability in the tropical atmosphere.

Where g is the acceleration due to gravity, T_{ve} and T_{vp} are the virtual temperatures of the environment and parcel, respectively. Z_{LNB} and Z_{LFC} are the heights of the level of neutral buoyancy and the level of free convection, respectively.

4.15 BRN

indicates the type of the thunderstorm: single, multicell, or supercell. (Weisman and Klemp, 1982, 1984)

$$\text{CAPE} / (0.5 \times U^2) = \text{BRN}$$

Where U is the magnitude of the shear?

5. DYNAMIC AND THERMO DYNAMIC CHARACTERISTICS

Thermodynamic indices were calculated for Machilipatnam from 7 May 12 z to 12 May 00 z, and the results Except for the 8th of May, 12 Z, we got a lifted index (more than the threshold value of -0.22 according to Khunz 2007). According to Schulz (1989), the sweat index exceeded the threshold value of >300 on May 10th-11th and 7th-8th, indicating the development of severe weather over Machilipatnam. The K index is greater than the threshold value of > 30 (according to Ackerman and

Knox). May 7th to 12th were observed. According to Haklander and Delden (2003), the total sum index is greater than 46.7, and the SST increased from May 7th to May 9th. CAPE is an indication of the instability of the atmosphere and can be used to assess the potential development of convection, which can lead to heavy rainfall, thunderstorms, and other severe weather. CAPE values greater than the threshold value of >897 (Mukhopadyay et al.2003) were observed on all days. The bulk Richardson number is greater than the threshold value, i.e., >40 was observed on all days except May 9th, 12 h to 11 h, and more was observed on the remaining days. Precipitable water is increasing throughout the day, and it reaches a peak on May 11th, when systems cross the coast. All the days A perceptible water parameter that indicates the onset of severe weather. Also, all of the days indicate that conditions are favourable for the development of atmospheric instability.

	07/12	08/00	08/12	09/00	09/12	10/12	11/00	11/12	12/00
Lifted index	-7.0	-8.2	0.33	-5.31	-3.71	-2.29	-1.35	-1.75	-1.27
Sweat index	333.8	376.1	217	261	282.6	386.6	356	311.6	290.42
K index	41.5	47.2	35.1	38.9	40.2	40.1	42.5	41	39.7
Total totals index	53.2	55.4	45.4	49.8	48.2	44.4	43.5	44.30	41.2
CAPE	2617.	2498.2	165.4	1367	1194.8	866.3	714.2	1970.9	880.3
CI	-251.7	-4.02	-296	-181.3	-119	-36.2	-92	-321	-1.73
EL	108	110.48	347.7	135.6	164.5	143.2	106	106	161.1
LFC	729.04	918.5	659	730.6	767.67	810.7	625	569	925.0
LCL	886.4	922.7	771	925	831	908.5	934	932	952.1
Bulk Richardson number	173	79.95	8.16	40.6	21.42	19.9	21.04	42.7	298
Precipitable Water(mm)	58.4	67.19	51.1	57.41	61.8	79.9	82.5	80.1	71.7

Table:1 Thermo Dynamic indices are calculated for the period from 7th May 12z to 12th May 00z of Machilipatnam station.

Threshold values for different parameters are given below

Lifted index (K)	≤-0.22 (Kunz 2007)
SWEAT	<-3 (Ackerman and Knox, online documentation) >300 (Schulz 1989) ≥134 (Haklander and Delden 2003)
K index	≥21(Peppler and Lamb1989. Andersson) ≥26.1(Kunz 2007) >30 (Ackerman and Knox)
Total totals index	≥46.7(Haklander and Delden 2003) ≥48.1(Kunz 2007) 48 (Ackerman and Knox)
CAPE	>896.8(Mukhopadyay et al.2003)
Bulk Richardson number(BRN)	>40 (onlone documentation)

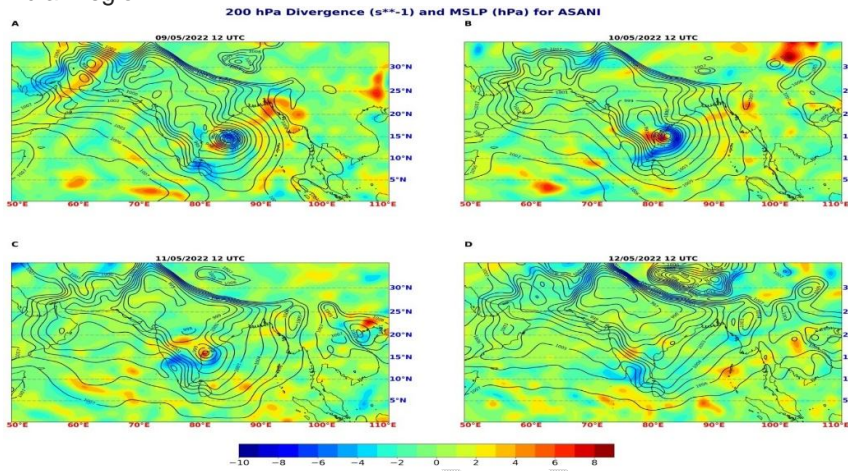
Table1a Threshold values for different Thermodynamic parameters

During cyclogenesis, tropical cyclones mainly depend on the sea surface heat flux and the vertical shear of the horizontal wind (De Maria, 1996). High SST plays a crucial role in enhancing deep convection by supplying necessary heat and moisture in the upward direction. At a given latitude, the rate of intensification increases with an increase in SST (Fig. 2A), on account of the significant increase in surface moisture fluxes from the warmer ocean (Crnivec et al., 2016). The low wind shear in an unstable stratified atmospheric environment allows the uniform upward and undisturbed release of the latent heat from the sea surface supporting the upper air supply, which was continued up to May 9th, but later SST gradually decreased, resulting in reduced heat fluxes. Fig.2 B,C,D SST in D is less than 260 degrees Celsius.Upper-level jets also play a crucial role in the

genesis and development of tropical cyclones. According to the Dines compensation principle, this divergence creates lower-level convergence above the sea surface, which helps vertical development above the sea surface. With the strengthening of the jet, this vertical development strengthens and pressure falls on the sea surface. Thus, upper-level jets help in the genesis of tropical cyclones. However, in this study, the jet supported storm intensification until May 9. Later, as the storm weakened due to left exit resulting in upward convergence and while proceeding towards the coast, the storm's height was limited to middle tropospheric levels. As a result, the system's steering changed.

The low pressure area was located in a more favourable region, with low vertical shear of horizontal wind and high SST (>31 °C) (Fig. 3 A), which served as an initial inducement environment for the cyclone's movement.

Divergence initially increased and peaked on May 9th and 10th, as shown by more concentric lines in fig. 3 (A, B) with more negative values; later, divergence decreased (C, D) with less negative values, as shown in fig. 1 (A-D). The subtropical westerly jet (STWJ) is generally located at 27–30°N in the Indian region.



• Fig1 200 Hpa Divergence and MSLP for Asani

Jet stream The right entrance was observed on May 9. Upper-level wind divergence, which continued through May 10, causes surface convergence, which causes intensification up to May 10 (Fig 3A-D). Later, as the jet left exit, upper level convergence caused surface level pressure to rise, causing the system to weaken by May 12.

Total column water vapour and total column Rainwater content increased on May 9 and then decreased as intensity and water vapour content decreased (Fig. 4 A-D). All the water vapour content is available on the west side of Machilipatnam. Total rainwater content increased until May 10, when it gradually decreased until there was negligible vapour content on May 12, 12 UTC. (Fig. 4 (A-D))

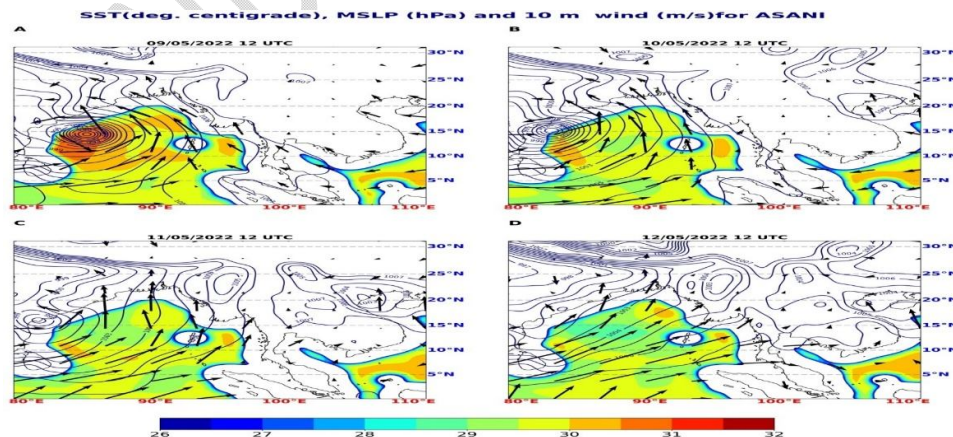


Fig2 SST(°C), MSLP (Hpa) and 10m wind (m/s) for ASANI

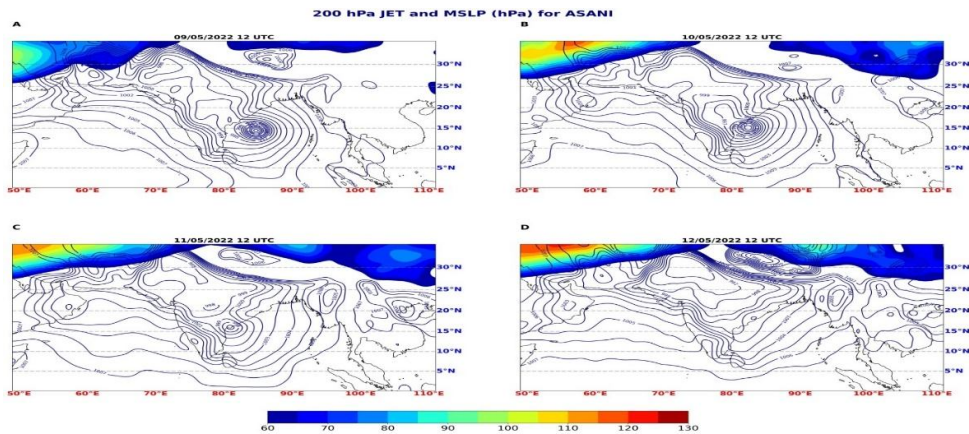


Fig:3 200hpa jet and MSLP hpa for Asani

Specific humidity during its intensification its content is more Fig 5(A-D) and once it met with cold waters the humidity levels also reduced leads to weakening of the system and moved west wards.

The upper level jet, steering flow (averaged wind fields between 850-300hpa to incorporate upper level trough ridge) guides Asani in its trajectory till landfall on the Machilipatnam coast Fig:6 (A-D). (Hanley et al., 2001) examined that tropical cyclones over warm water and away from coast are more likely to

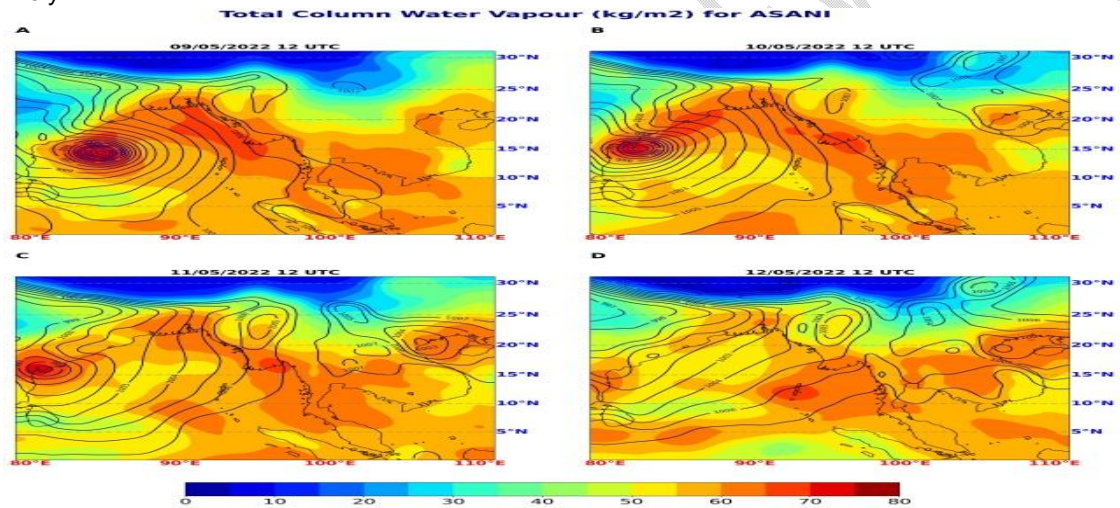


Figure 4 shows the total column water vapour (Kg/m2).

intensify rather than weaken after interaction with an upper-level trough. In this study, a tropical cyclone passing over less warm water and close to the coast for a day caused the system to weaken due to interaction with an upper level trough. Fig7

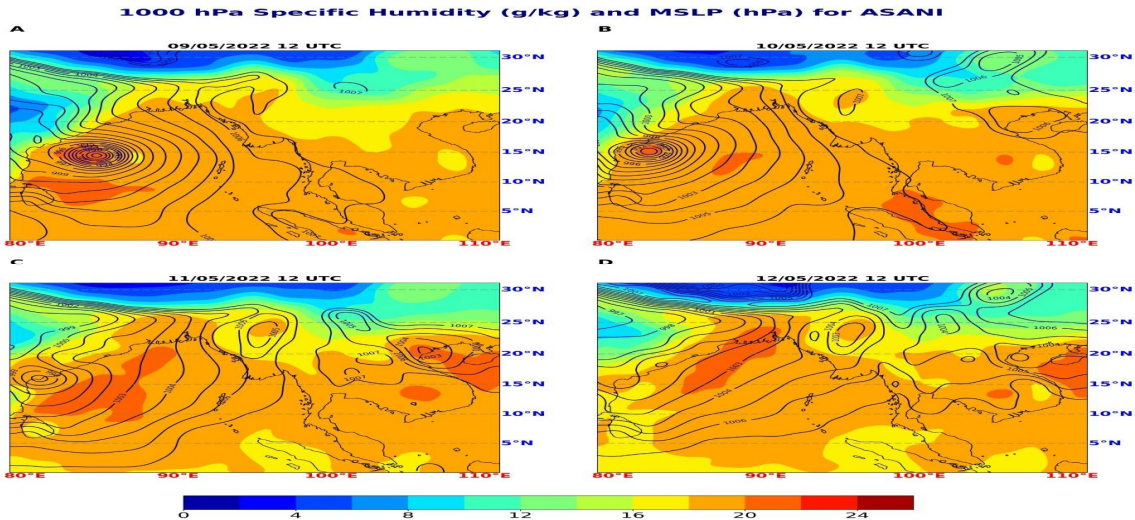


Fig:5 1000hpa specific humidity (g/Kg) and MSLP in hpa.

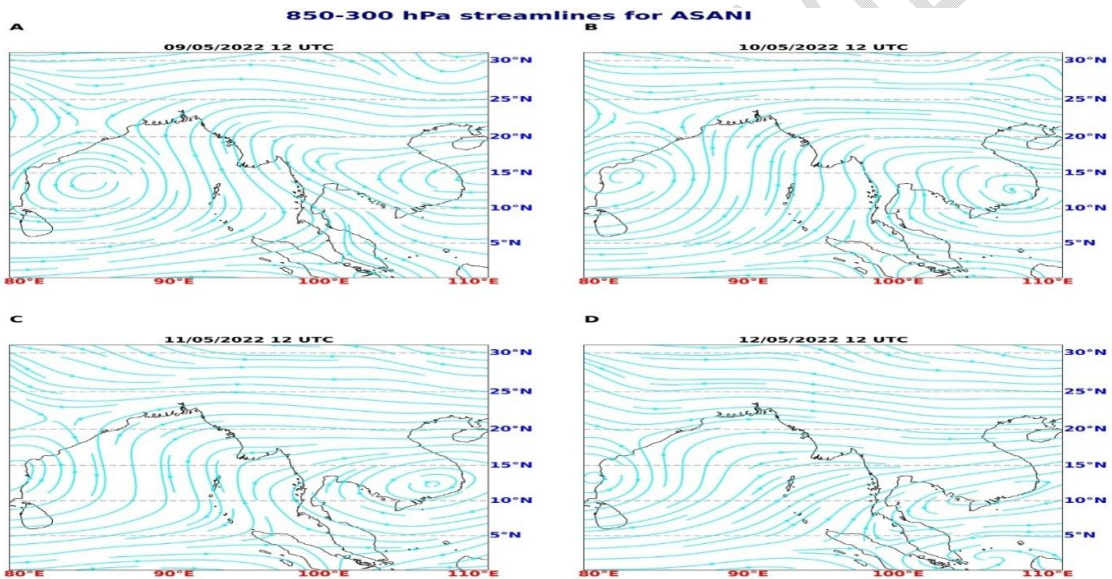


Figure 6: Asani stream line from 850 to 300 hpa.

The time evolution of STWJ and the system is shown in Fig. 2 200 hpa wind and MSLP. Figure 2 shows how, over time, STWJ strengthen and isobars become more closely spaced. This STWJ is associated with upper-level divergence (fig. 1) and lower-level convergence (relative vorticity in SST fig. 10). This is also evident from the vertical profile of divergence shown in Fig. 1. The presence of upper level divergence increases lower level convergence, which increases instability and favours intensification up until May 10; at that point, Asani becomes a severe cyclonic storm, but its direction changes due to the position of the upper level ridge, Figs 13a; it moved slowly northward or north-westward on May 11 until the evening, and then slowly west-south-westward thereafter. It was mainly due to the fact that the cyclonic storm was supposed to move northeastward near the coast under the influence of a short-amplitude westerly trough in the middle and upper troposphere that proceeded from the west. However, as the storm weakened as it moved closer to the coast, its height decreased, limiting it to middle tropospheric levels. As a result, the storm's steering wind shifted from being dominated by southerly winds to leading to north-westward movement. However, the northward movement was restricted or blocked due to an anticyclone lying over the peninsula of India (figs. 13b). As a result, the system moved slowly and remained practically stationary near the coast, followed by

slow west-southwestward movement until it weakened into a well-defined and low-pressure area over the region in the morning of May 12.

The magnitude of sensible Latent heat flux is governed by the difference in temperature between the surface and the overlying atmosphere, wind speed, and surface roughness. Surface latent heat flux is the transfer of latent heat between Earth's surface (land or ocean) and the atmosphere through the effects of turbulent air motion. Evaporation from the Earth's surface represents a transfer of energy from the surface to the atmosphere. (Emanuel, 1986) proposed that "interaction and maintenance of tropical cyclones depend exclusively on self-induced heat transfer from the ocean" via surface heat fluxes. (Wing *et al.*, 2019) also argued that strong feedback from surface heat fluxes such as surface latent heat flux and surface sensible heat flux can intensify tropical cyclones.

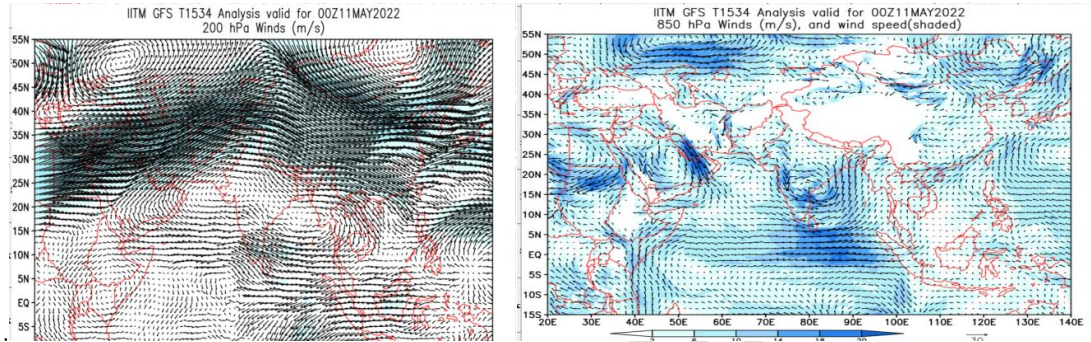


Fig:7 IITM GFS T1534 wind analysis for 11th May at 200hpa(a) and 850 hpa(b) level

Latent heat flux exchanges at the air-sea interface play important roles in the formation and development of tropical cyclones. It is a fundamental source of energy for tropical cyclones (Ma *et al.*, 2015). Fig. 8 (A-D) shows that latent heat fluxes are more negative during the intensification process once the SST decreases in the sea and the system meets with cold waters. Latent heat decreases. lead to system weakening.

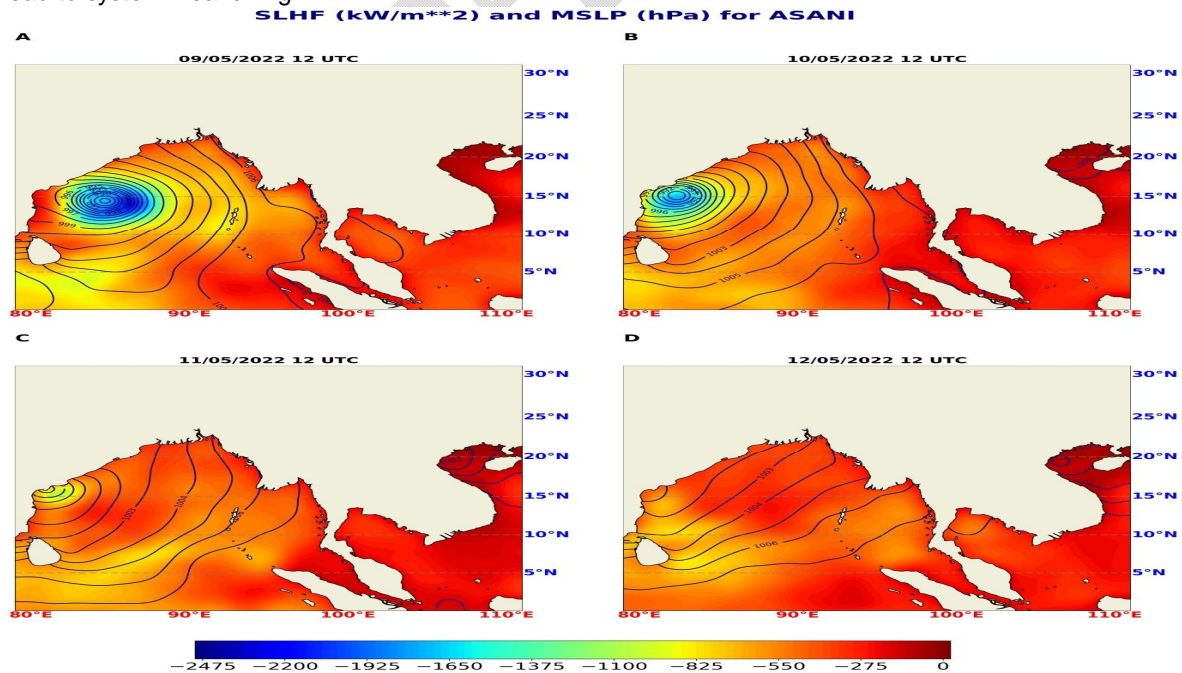


Fig 8 Sensible latent heat flux

The magnitude of sensible heat flux is governed by the difference in temperature between the surface and the overlying atmosphere, wind speed, and surface roughness. Surface heat fluxes are positive downwards and negative upwards. According to Fig. 9, the surface sensible heat flux is greater on

May 9th and for any system during intensification is negative upwards (A, B), and later days positive values indicate system weakening, as shown in Fig. 9 C, D.

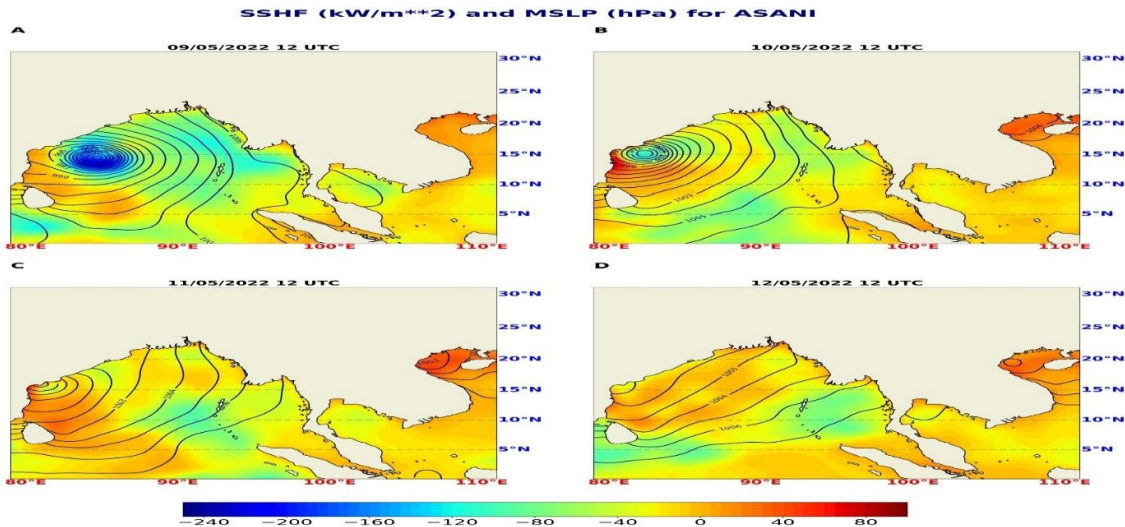
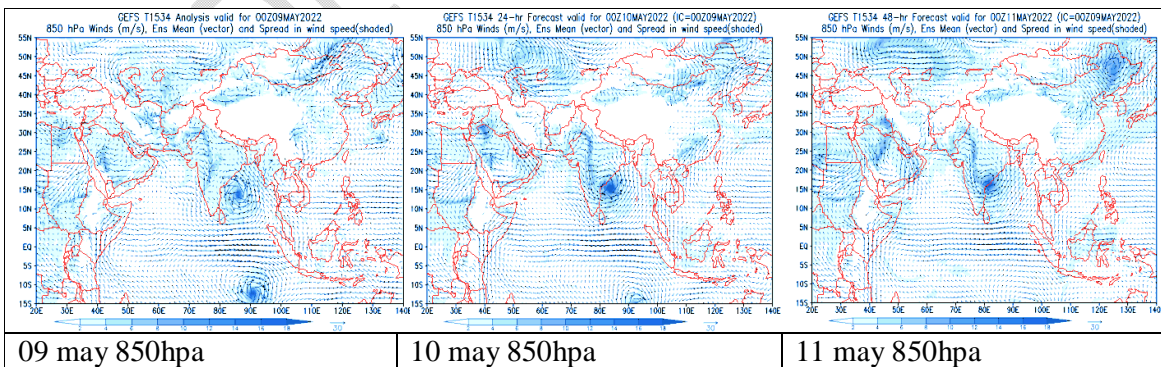


Fig:9 Surface sensible heatflux and MSLP hpa

Sea surface temperature (SST) was around 30–31°C for the entire bob. It decreases gradually toward the Andhra Pradesh and Odisha coasts, becoming 28°C. The ocean heat content (OHC) is greater than 100 kJ/cm² over the west central and south bays of Bengal (Bo), but drops to 50-70 kJ/cm² along and off the coasts of Andhra Pradesh and Odisha, and adjoining the west central bob. IMD predicts that low-level vorticity is about $250 \times 10^{-6} \text{ s}^{-1}$ to the south of the system center. Vertically, it can reach 200 hpa. The vorticity field is east-west oriented, indicating gradual westward vorticity advection. Low-level convergence is around $10 \times 10^{-5} \text{ s}^{-1}$ to the southwest of the system centre. Upper-level divergence is $05-10 \times 10^{-5} \text{ s}^{-1}$ to the northeast of the system centre. Wind shear is low (10–15 knots) (IMD RSMC website) around the system area and also along the forecast track. As the system moves further northward, it will encounter lower SST and OHC and hence show gradual weakening. As the system moves further north, dry air will infiltrate the core area from the Indian landmass. It will contribute to the system's demise. Instead of recurving northeastwards, the system moved north-westward and, after crossing the coast, moved in a south-west direction while moving along the periphery of the sub-tropical ridge associated with anticyclonic circulation over the east-central Bay of Bengal.



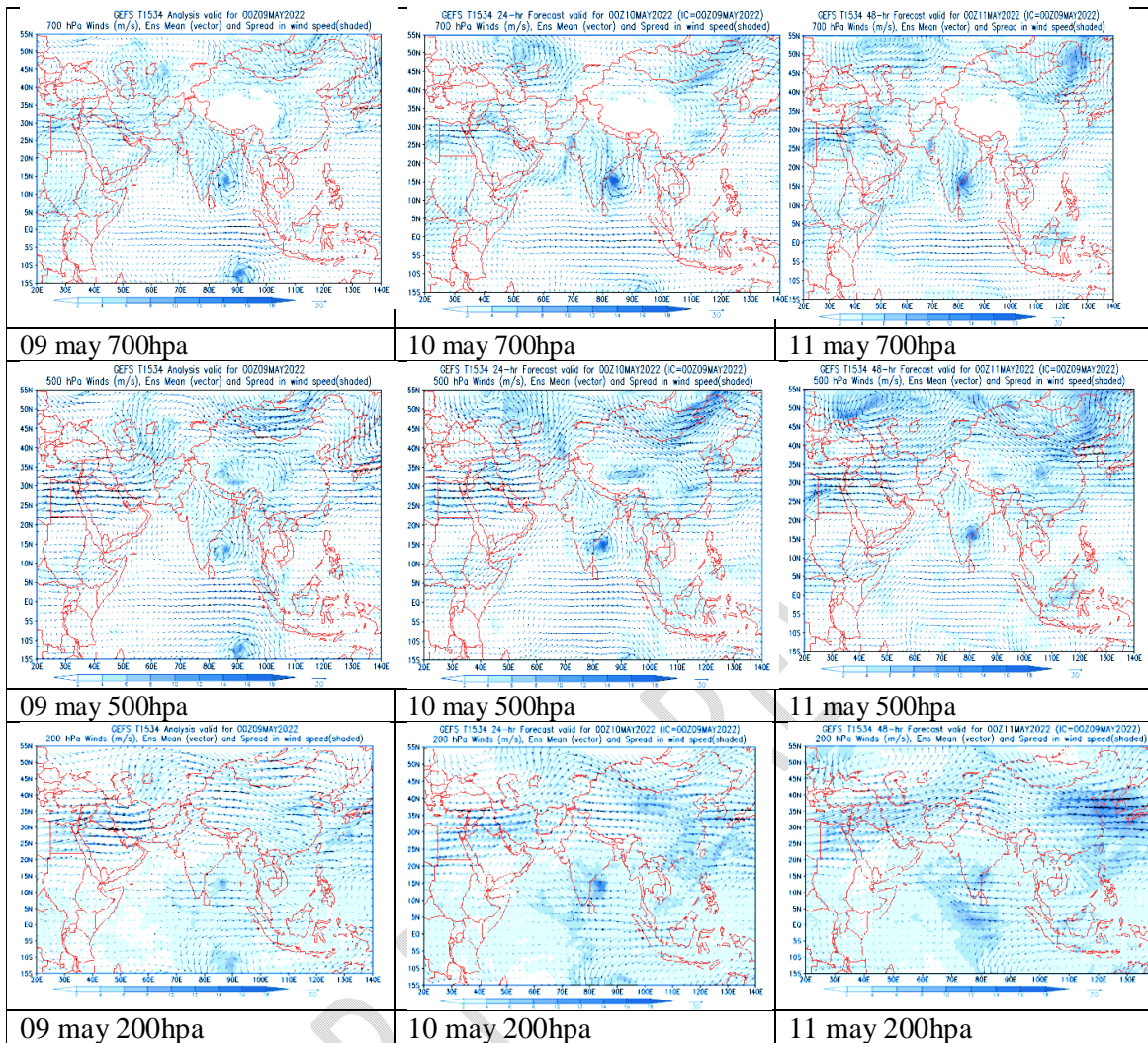


Fig 10 GEFS Wind Analysis At 850,700,500 And 200hpa

11th, 1200 UTC sea surface temperature (SST) is around 29 oC over west-central India, along and off Andhra Pradesh, and along the forecast track. The ocean heat content (OHC) over the west-central and south bays of Bengal (Bod) is 100 KJ/cm², and 50-70 KJ/cm² over the northwest bob along and off the coasts of Andhra Pradesh and Odisha, as well as adjoining the west-central bob. Low-level vorticity has decreased and is now around 150 x 10⁻⁶ s⁻¹ to the south of the system centre (RSMC IMD bulletins). Vertically, it can reach 200 hpa. Low-level convergence has slightly increased and is around 20 x 10⁻⁵ s⁻¹ to the southwest of the system center. Upper-level divergence is 05 x 10⁻⁵ s⁻¹ around and to the northeast of the system centre. Wind shear is low (15–20 knots) around the system area and also along the forecast track. Because of land interactions, the system has weakened and will continue to weaken gradually. Also, as the system moved further west-northwestward, it encountered lower SST and lower OHC and hence weakened. The incursion of cold and dry wind from the Indian Peninsula from the middle and upper troposphere also contributed to the weakening of the system.

The 11th of May, 1800 (RSMC IMD bulletins)

The sea surface temperature (SST) is around 29 degrees Celsius over westcentral Bob, along and off the coast of Andhra Pradesh. The ocean heat content (OHC) is 100 kJ/cm² over the west central and south bays of Bengal (Bod), then drops to 50-70 kJ/cm² over the northwest Bod, along and off the coasts of Andhra Pradesh and Odisha, and adjacent West Central Bod. Low-level vorticity has decreased and is about 150 x 10⁶ s⁻¹ to the south of the system centre. Vertically, it can reach 200 hpa. To the northwest of the system center, low-level convergence is approximately 30 x 10⁻⁵ s⁻¹. Upper-level divergence is 05 x 10⁻⁵ s⁻¹ around to the southwest of the system centre. Wind shear is

low (15-20 knots) in the system's vicinity. The system weakened due to land interactions and will weaken further gradually.

6. Weather observations: 1. The highest rainfall of 256.4 mm was recorded in Kandukur (Prakasam District) in Andhra Pradesh in 24 hours ending at 0830 hrs IST on May 12th, 2022. Winds: Gale Winds of 75–85 kmph (40–45 kts) gusting to 95 kmph (50 kts) were experienced around the system centre over the west-central Bay of Bengal on the 11th morning, and 65–75 kmph (35–40 kts) over the land. A maximum wind of moderate intensity of 39 kmph (21 kts) from a south-easterly direction was experienced at Machilipatnam at 1600 UTC (2130 Damages caused by winds in association with a storm over land were minimal or very minimal.

3. The worst affected areas due to rain were the southern coastal strip of Prakasam and the northern coastal strip of Nellore districts, where 20 to 30 cm of average rainfall was recorded in three days (May 11–13).

6.1 Wind Direction Before and After Passage of a Low Pressure System at a Station

When a low-pressure system or cyclone approaches a station along the coast from the sea, winds will blow from the northeast or east if the centre of the system is to the south of the station. After the centre has passed, inland winds will veer and blow from the east or southeast. If the centre is to the north of the station, winds will blow from the northwest or west before crossing, then reverse and blow from the southeast.

southwest or south after crossing. If the centre passed directly over the station, the wind would first blow from the north or northeast, become calm or very light during the passage of the centre (or eye), and blow from the southwest or south afterwards.

6.2 LANDFALL POINT FIXING AND SYSTEM MOVEMENT IN SOUTHWESTERN DIRECTION OVER LAND

Hourly weather observations recorded at coastal observatories along the Andhra Coast are considered in assessing the landfall point and movement of the system thereafter (Fig. 11). At Machilipatnam, northerly winds prevailed in the morning of May 11, 2022, and they veered and became northeasterly by afternoon. They then became easterly (10 kt) at 1400 UTC (1930 hrs IST). At that hour, the station recorded the lowest pressure of 994.9mb along the Andhra Coast. By 1500 UTC (2030 hrs IST), the wind had shifted to the south. It clearly indicates that the Deep Depression crossed the coast south of Machilipatnam and very close to it. It is further supported by the fact that at Bapatla on the 11th, northwesterly winds had been blowing since the morning and were west-northwesterly 5 kt at 1500 UTC (Fig. 11), indicating wind backing and the system being located to the north of the station. Based on the above synoptic features and fixing the centre of the system by means of drawing lines at an angle of 120° to the direction of wind observed at stations and the centroid position of lines at 1400 and 1500 UTC, it can be well assessed.

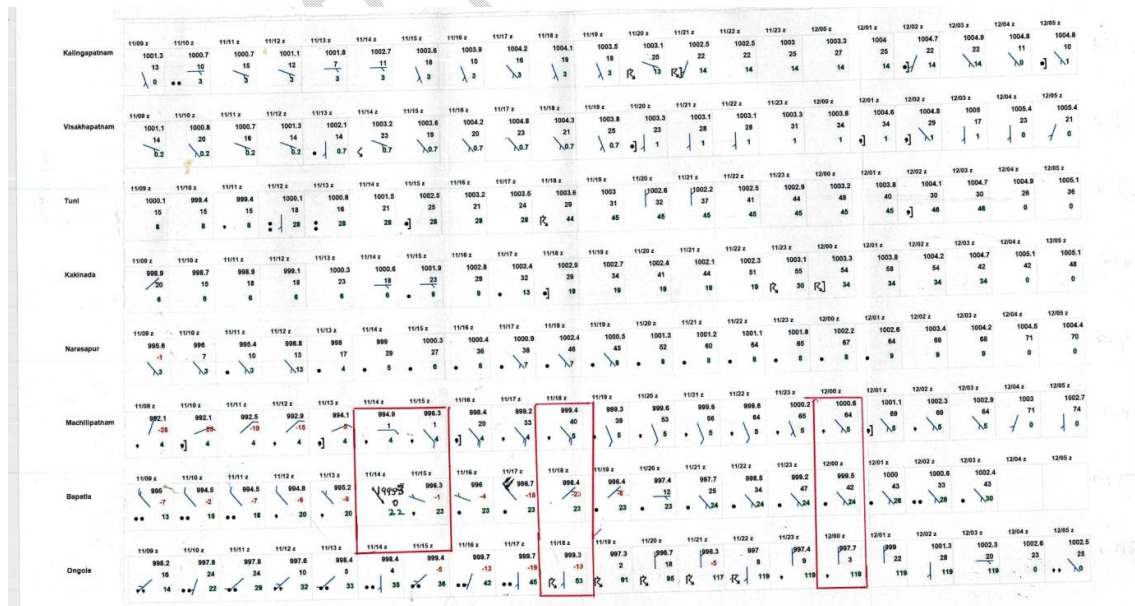


FIG. 11: HOURLY OBSERVATIONS RECORDED OVER COASTAL ANDHRA PRADESH OBSERVATORIES

It is a rare occurrence that a low-pressure system moves in a south-westerly direction after making landfall. In the present case, the system, after crossing the coast in its weakening stages of depression and low pressure, moved near Machilipatnam in a south-westerly direction over coastal areas of Guntur, Prakasam, and Nellore Districts on May 11 and 12, 2022 (Fig. 12). A similar case of south-westerly movement after landfall occurred in the year 1984. In the afternoon of November 14, 1984, a severe cyclonic storm with a core of cyclonic winds crossed the south Andhra Coast just north of Sriharikota. After crossing the coast, the system slowly moved in a south-westerly direction and rapidly weakened into a cyclonic storm by 14th evening and into a depression by 15th morning, then fizzled out thereafter.

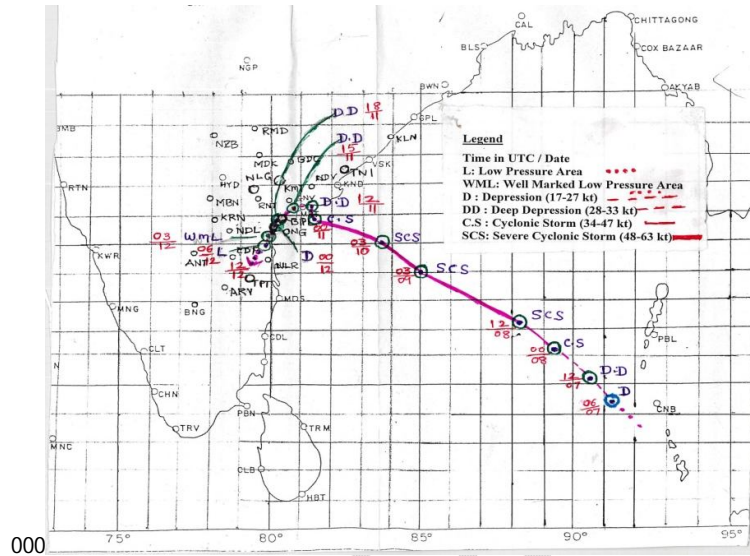


Fig :12 Observed track of SCS Asani Cyclone

Benefits:

Due to the passage of cyclonic storm people in Andhra Pradesh experienced relief from scorching hot weather from 10 to 13th May 2022, as thick cloud canopy protected them from hot sun rays. The maximum temperatures recorded were markedly below normal by 5 to 14°C over Andhra Pradesh during the above period. Due to Upwelling of seawater led to off south coastal Andhra Pradesh became a potential fishing zone with this system.

Conclusion:

- 1.The observations of the synoptic and dynamical parameters associated with SCS Asani clearly show that the formation of SCS Asani was aided under favourable conditions of high SST, high energy, weak wind, vertical shear of horizontal wind, and 200 hpaSTWJ.The violent cyclonic storm "Asani" deteriorated into a deep depression before reaching the shore, owing to a drop in sea surface temperature and heat content in the water. It travelled slowly toward the shore (5-6 kph compared to the average pace of 13 kph) and stayed within 50 km of the coast from the morning until the evening of May 11th. The sluggish movement caused upwelling of sea water and rainfall over the sea, which resulted in additional cooling of the sea surface. Because of the slow movement, there was more time for land interaction, which resulted in weakening owing to relatively high friction with the land surface. There was cold and dry air intrusion from the Indian landmass in the middle and upper tropospheres, which is unfavourable for any cyclonic storm's tenacity.
- 2.Because the cyclonic storm was expected to proceed north-eastwards along the coast under the influence of a short-amplitude westerly trough in the middle and upper tropospheric levels arriving from the west, it moved west-southwest. However, when the storm weakened as it approached the shore, its height fell, limiting it to the middle tropospheric regions. As a result, the storm's steering wind shifted from being dominated by south-easterly winds to being dominated by north-westerly winds, causing it to proceed north-westward. However, the northward movement was restricted or blocked due to an anticyclone over peninsular India. Thus, the system moved slowly and stayed nearly stationary along the shore until weakening into a well-defined low pressure area in the morning of May 12.
- 3.The coastal winds that are caught up in the cyclonic circulation of low-pressure systems determine the landfall site and migration of low-pressure systems across land (normally about 150 to 200 km

away from the coast). It is a well-established fact that micro-scale variations in wind and pressure are the primary ingredients, or play a critical role, in determining landfall position and the continued movement of the low-pressure system over land. Satellite and radar cloud images serve an auxiliary role in system forecasting over land areas.

4. It is an unusual phenomenon when a low-pressure system (the remnant of Asani) moves in a south-westerly direction after its landfall.

Abbreviations

RSMC	:	Regional specialised Meteorological centre
ECMWF	:	European Centre for Medium Range Forecast
BoB	:	Bay of Bengal
MSLP	:	Mean Sea Level Pressure
CAPE	:	Convective available Potential Energy
SST	:	Sea Surface Temperature
STWJ	:	Sub Tropical Westerly Jet

References

- Andersson T, Andersson M, Jacobsson C, Nilsson S (1989) Thermodynamic indices for forecasting thunderstorms in southern Sweden. *Meteorol Mag* 116:141–146
- Chinchole, P. S. and Mohapatra, M., 2017, "Some characteristics of Transitional Speed of Cyclonic Disturbances Over north Indian Ocean in Recent Years", *Tropical Cyclone activity over the North Indian Ocean*, Ed. Mohapatra, M., Bandyopadhyay, B. K. and Rathore, L. S., Co-published by Capital Publishers, New Delhi and Springer, Germany, 165-179.
- Čranivec, N., Smith, R. K. and Gerard, Kilroy, 2016, "Dependence of tropical cyclone intensification rate on sea-surface temperature", *Q. J. R. Meteorol. Soc.*, **142**, 1618-1627.
- De Maria, M., 1996, "The effect of vertical shear on tropical cyclone intensity change", *J. Atmos. Sci.*, **53**, 2076-2087.
- Emanuel, K.A., 1986, "An air-sea interaction theory for tropical cyclones. Part I: Steady-state maintenance", *J. Atmos. Sci.*, **43**, 585-605.
- George JJ (1960) Weather forecasting for aeronautics. Academic press, 411 pp
- Gray, W. M., 1968, "Global view of the origin of tropical disturbances and storms", *Mon. Wea. Rev.*, **96**, 669-700.
- Hanley, D., Molinary, J. and Keyser, D., 2001, "A composite study of the interactions between tropical cyclones and upper-tropospheric troughs", *Mon. Wea. Rev.*, **129**, 2570-2584
- Haklander AJ, Delden AV (2003) Thunderstorm predictors and their forecast skill for The Netherlands. *Atmos Res* 67–68:273–299
- Hersbach, H. and Dee, D., 2016, "ERA5 reanalysis in production", *ECMWF Newsl.lett.*, **147**, 7.
- Kunz M (2007) The skill of convective parameters and indices to predict isolated and severe thunderstorms. *Nat Hazards Earth Syst Sci* 7:327–342
- Li, T. and Fu, B., 2006, "Tropical Cyclogenesis Associated with Rossby Wave Energy Dispersion of a Preexisting Typhoon. Part I: Satellite Data Analysis", *J. Atmos. Sci.*, **63**, 1377-1389.
- Ma, Z., Fei, J., Huang, X. and Cheng, X., 2015, "Contributions of surface sensible heat flux to tropical cyclone. Part I: Evolution of Tropical cyclone intensity and structure", *J. Atmos. Sci.*, **72**, 120-140.
- Means LL (1952) Stability index computation graph for surface data. Unpublished manuscript available from F. Sanders, 9 Flint St., Marblehead, MA 01945, 2 pp
- Manganello, J. V., K. I., Hodges, Kinter, J. L. III., Cash, B. A., Marx, L., Jung, T., Achuthavari, D., Adams, J. M., Altshuler, E. L., Huang, B., Jin, E. K., Stan, C., Towers, P. and Wedi, N., 2012, "Tropical cyclone climatology in a 10-km global atmospheric GCM: toward weather-resolving climate modeling", *J. Clim.*, **25**, 11, 3867-3893.
- Miller R (1972) Notes on analysis and severe storm forecasting procedures of the Air Force Global Weather Central. Technical Report 200 (Rev.), AWS, U.S. Air Force (Headquarters, AWS, Scott AFB, IL 62225), 102 pp
- Mohapatra, M., Bandyopadhyay, B. K., Ray, Kamaljit and Rathore, L. S., 2014b, "Early Warning Services for Management of Cyclones over North Indian Ocean: Current status and future scope, High Impact Weather Event over SAARC Region", Ed. Ray, Kamaljit, Mohapatra, M.,

Bandyopadhyay, B. K. and Rathore, L. S., Capital Publishing Co. and Springer Publications Ltd.

Moncrieff M, Miller M (1976) The dynamics and simulation of tropical cumulonimbus and Squall lines. *QJR Meteorol Soc* 102:373–394

Montgomery, M. T. and Farrell, B. F., 1993, "Tropical Cyclone Formation", *J. Atmos. Sci.*, **50**, 285–310.

Mukhopadhyay P, Sanjay J, Singh SS (2003) Objective forecast of thundery/non thundery Days using conventional indices over three northeast Indian stations. *Mausam* 54(4):867–880

Palmén, E., 1948, "On the formation and structure of tropical hurricanes", *Geophysica*, **3**, 26–39.

Peppler RA, Lamb PJ (1989) Tropospheric static stability and central North American Growing season rainfall. *Mon Weather Rev* 117:1156–1180

Pielke, R. A. and Pielke, R. A. S., 1997, "Hurricanes: Their Nature and Impact on Society", John Wiley and Sons, p279.

Poddar, S., Mondal, M. and Ghosh, S., 2020, "A Survey on Disaster: Understanding the After effects of Super Cyclone Amphan and Helping Hand of Social Media", *arXiv*, arXiv:2007.14910v1[cs.CY] 29th July, 2020.

Ramage, C. S., 1959, "Hurricane development", *J. Meteorol.*, **16**, 227–237.

Sadler, J. C., 1976, "A role of the tropical upper tropospheric trough in early season typhoon development", *Mon. Wea. Rev.*, **104**, 1266–1278.

Sanap, S. D., Mohapatra, M., Ali, M. M., Priya, P. and Varaprasad, D., 2020, "On the dynamics of cyclogenesis, rapid intensification and recurvature of the very severe cyclonic storm, Ockhi", *J. Earth, Syst. Sci.*, **129**, p194.

Schulz P (1989) Relationships of several stability indices to convective weather events in northeast Colorado. *Weather Forecast* 4:73–80.

Simpson, R., Anthes, R. A. and Garstang, M., 2002, "Hurricane! Coping with Disaster: Progress and Challenges since Galveston", *Amer. Geophys. Union*, p360.

Wang, Y., Davis, C. A. and Huang, Y., 2019, "Dynamics of Lower-Tropospheric Vorticity in Idealized Simulations of Tropical Cyclone Formation", *J. Atmos. Sci.*, **76**, 707–727.

Weisman ML, Klemp JB (1982) The dependence of numerically simulated convective storms on vertical wind shear and buoyancy. *Mon Weather Rev* 110:504–520

Weisman ML, Klemp JB (1984) The structure and classification of numerically simulated convective storms in directionally varying wind shears. *Mon Weather Rev* 112:2479–2498.

Williams, E., and N. Renno (1993), an Analysis of the conditional instability of the tropical atmosphere, *Mon, Weather Rev.*, 121, 21–36.

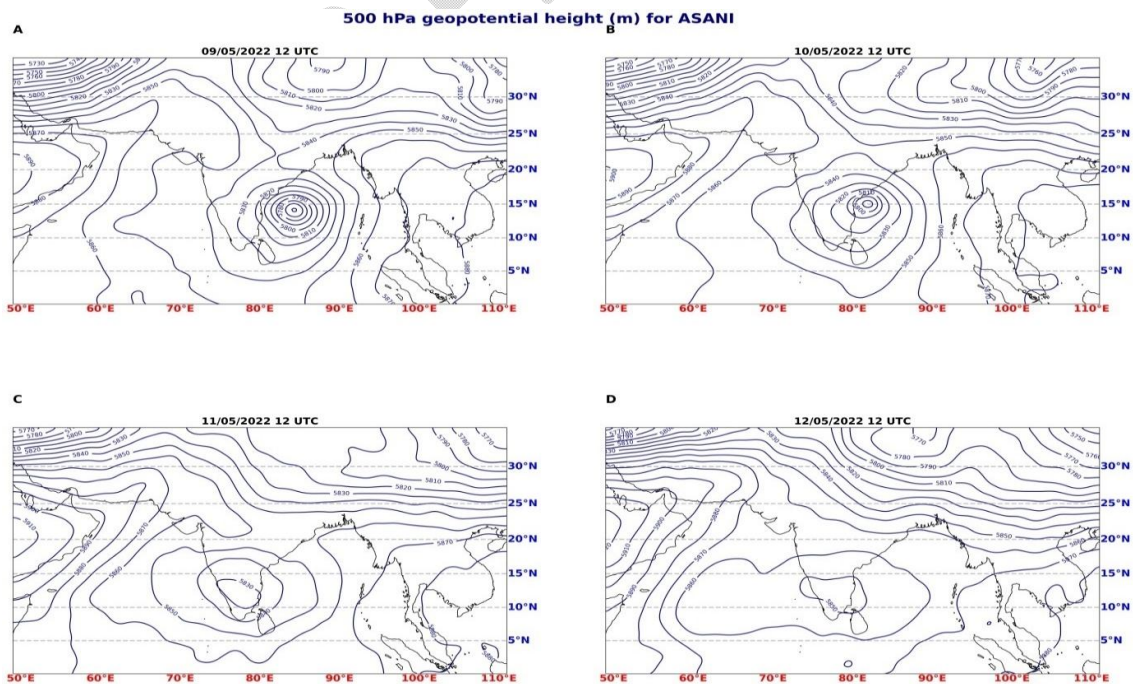


Fig: 13 500hpa geopotential height for Asani

UNDER PEER REVIEW